ChemPubSoc Europe

DOI: 10.1002/chem.201701204

CHEMISTRY A European Journal Full Paper

Fluorophosphates

Benzyl Mono-*P*-Fluorophosphonate and Benzyl Penta-*P*-Fluorophosphate Anions Are Physiologically Stable Phosphotyrosine Mimetics and Inhibitors of Protein Tyrosine Phosphatases

Stefan Wagner, Matteo Accorsi, and Jörg Rademann*[a]

Abstract: α,α-Difluoro-benzyl phosphonates are currently the most popular class of phosphotyrosine mimetics. Structurally derived from the natural substrate phosphotyrosine, they constitute classical bioisosteres and have enabled the development of potent inhibitors of protein tyrosine phosphatases (PTP) and phosphotyrosine recognition sites such as SH2 domains. Being dianions bearing two negative charges, phosphonates, however, do not permeate membranes and thus are often inactive in cells and have not been a successful starting point toward therapeutics, yet. In this work, benzyl phosphonates were modified by replacing phosphorus-bound oxygen atoms with phosphorus-bound fluorine atoms. Surprisingly, mono-*P*-fluorophosphonates were fully stable under physiological conditions, thus enabling the investigation of their mode of action toward PTP. Three alternative scenarios were tested and mono-*P*-fluorophosphonates were identified as stable reversible PTP1B inhibitors, despite of the loss of one negative charge and the replacement of one oxygen atom as an H-bond donor by fluorine. In extending this replacement strategy, α,α-difluorobenzyl penta-*P*-fluorophosphates were synthesized and found to be novel phosphotyrosine mimetics with improved affinity to the phosphotyrosine binding site of PTP1B.

Introduction

Phosphorylation and dephosphorylation of proteins at serine, threonine, and tyrosine residues are major natural mechanisms of activation or deactivation of biomacromolecules. Not surprisingly, protein tyrosine, serine, and threonine phosphatases have been postulated as valuable pharmacological targets.[1–3] However, no phosphatase inhibitors have been admitted as drugs for clinical use so far. For these reasons, novel chemical tools for the detection and modulation of phosphatase activity are still in high demand.[4]

Most protein tyrosine phosphatase (PTP) inhibitors compete with the phosphate substrate for the active site of the enzymes and thus contain phosphate bioisosteres, which can be developed to highly specific inhibitors by extension with fragments targeting specific secondary binding sites.[5–7] Bioisosteres of the phosphotyrosine residue include benzyl phosphonates,[8] difluorobenzyl phosphonates,[9,10] sulfonates,[11,12] triflylamides,[13] carboxylic acids,[14,15] and isothiazolidinones.[16,17] Recently, benzoyl phosphonates were discovered as photoactivated phosphotyrosine bioisosteres and have been used for the specific deactivation and covalent labeling of phosphotyrosine recognition domains[18] and photo-deactivation of PTP.[19] Other chemically reactive inhibitors blocking and deactivating the catalytic site of the enzyme in a mechanism-based reaction have been reported.[20,21] In addition, the development of covalent modifiers targeting the active sites of PTPs as "activity-based probes" has been pursued.[22–25]

Mono-*P*-fluorophosphonate esters have been described first in the 1930s on the search for insecticides and some compounds of this class were found to be highly toxic to humans. Subsequently, the mono-*P*-fluoromethylphosphonate esters sarin, cyclosarin, and soman were developed as chemical warfare agents.[26,27] Toxicity of these fluorinated phosphonate esters has been attributed to the inhibition of synaptic acetylcholine esterase.[28] Related *P*-fluorophosphate and phosphonate esters have been studied and found application as unspecific inhibitors and activity-based probes of serine hydrolases including proteases, lipases, and esterases.[29–32]

Results and Discussion

Despite the numerous reports on bioactivities of mono-*P*-fluorophosphonate esters, no results on the bioactivity or on the chemical stability of *P*-fluorinated benzyl phosphonates have been published so far. Therefore, starting from the well-known phosphotyrosine mimetics **1**–**3**, we decided to investigate the synthesis and the bioactivity of a series of mono-*P*-fluoro-

[a] Dr. S. Wagner, M. Accorsi, Prof. Dr. J. Rademann
Institute of Pharmacy, Medicinal Chemistry
Freie Universität Berlin
Königin-Luise-Str. 2+4, 14195 Berlin (Germany)
E-mail: joerg.rademann@fu-berlin.de

Supporting information and the ORCID identification number(s) for the author(s) of this article can be found under https://doi.org/10.1002/chem.201701204.

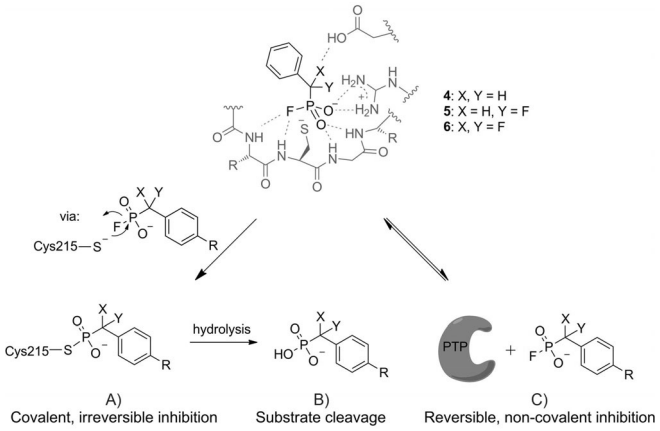

Figure 1. Benzyl-mono-*P*-fluorophosphonates **4**–**6** are phosphotyrosine mimetics derived from phosphonates **1**–**3**. They were investigated for three alternative modes of action toward PTP1B: A) as covalent, irreversible inhibitors, B) as substrates, or C) as reversible, non-covalent inhibitors.

phosphonates **4**–**6** (Figure 1).[8–10] We presumed these compounds to bind to the active site of the model enzyme PTP1B in a similar way as displayed in published crystal structures of this protein in complex with phosphonate inhibitors.[33–35] Numerous predicted charge and hydrogen bond interactions between compounds **4**–**6** and amino acid residues of the active site suggested non-covalent and eventually covalent interactions between the fragments and the target enzyme, possibly resulting in biological activity. Aim of our experiments was to evaluate the nature of this hypothetical bioactivity by testing three alternative scenarios (Figure 1 A)–C)). According to scenario A) compounds **4**–**6** could act as irreversible covalent inhibitors of PTP1B similar to mono-*P*-fluorophosphonate esters. They react with the active site of the enzyme, presumably by the attack of the thiolate of Cys215 at the phosphorus atom resulting in the cleavage of the P—F bond. This scenario is supported by the experimental findings demonstrating that thioesters of phosphonate **1** are chemically stable entities (see Figure S3 in the Supporting Information). In scenario B) mono-*P*-fluorophosphonates might act as substrates of PTP1B forming a covalent intermediate with the active site of the enzyme, which is subsequently hydrolyzed as part of a catalytic cycle. In scenario C) compounds **4**–**6** are stable phosphotyrosine mimetics acting as reversible, non-covalent inhibitors.

Synthesis of benzyl mono-*P*-fluorophosphonates

For a practical synthesis of the target compounds, we established that mono-*P*-fluorophosphonates were accessible directly from the phosphonic acids **1**–**3** using oxalyl fluoride as a powerful and efficient reagent (Scheme 1).[36] Oxalyl fluoride was superior to other fluorinating reagents like diethylaminosulfur trifluoride (DAST) and fluoride–chloride exchange reactions because it delivered pure products by evaporation of the excess of volatile reagent and byproducts. Intermediary di-*P*-fluorophosphonates were then converted to the targeted monofluorides **4**–**6** by the addition of water (Scheme 1).

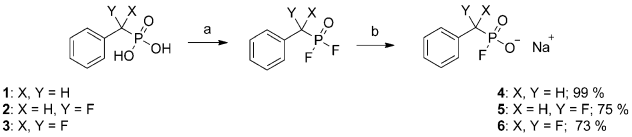

Scheme 1. Synthesis of benzyl mono-*P*-fluorophosphonate anions **4**–**6**. Reaction conditions: a) $(COF)_2$, acetonitrile; b) 1. H_2O, 2. Na-Amberlite.

Although the protonated, acidic forms of **4**–**6** were only partially stable in aqueous solution, ion exchange to the sodium salts yielded molecules that were significantly more stable in this environment and could be stored as solids for at least several months at 4 °C. The sodium mono-*P*-fluorophosphonates were also stable under HPLC-MS conditions (0.1 % formic acid in acetonitrile/water mixtures) and are retained by C-18 reverse-phase significantly stronger than their phosphonic acid derivatives (e.g., 4.0 min for **1** vs. 5.6 min for **4,** see Figure S1 in the Supporting Information).

In buffer solution at pH 7, no degradation of these compounds could be observed, whereas strongly basic conditions like 1 % (*w/v*) NaOD led to immediate hydrolysis. The mono-*P*-fluorophosphonate anions **4**–**6** were completely stable for several hours in buffer under mildly acidic and basic conditions at pH 5 and 9. Importantly, benzyl mono-*P*-fluorophosphonate **4** was entirely stable in the presence of 1 mM of dithiothreitol (DTT), the reducing agent conventionally used for the stabilization of protein tyrosine phosphatases in buffer and which is known to react with strong electrophiles (see Figure S2 in the Supporting Information)

All compounds were fully characterized by ^{1}H, ^{13}C, ^{19}F, and ^{31}P NMR spectroscopy. Characteristic signals of compound **6** in the ^{19}F NMR include the P-bonded fluorine at −75.6 ppm [relative to the standard trifluoroacetic acid (TFA)] with a $^{1}J_{P\text{-}F}$ coupling of 1035 Hz, and the phosphorus at 2.7 ppm in the ^{31}P NMR with a $^{2}J_{P\text{-}F}$ coupling of 114 Hz resulting in a doublet-triplet signal (Figure 2).

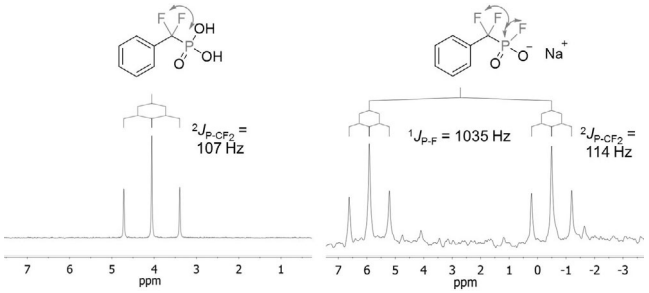

Figure 2. ^{31}P NMR spectra of the phosphonic acid **3** (162 MHz, [D6]DMSO, left) and the mono-*P*-fluorophosphonate **6** (162 MHz, D_2O, right) indicating the additional *ipso* $^{1}J_{P\text{-}F}$ coupling and the modified geminal $^{2}J_{P\text{-}CF2}$ coupling in **6**.

Biochemical evaluation of benzyl mono-*P*-fluorophosphonates

Next, the biological activity of the *P*-monofluorides was investigated. Enzymatic activity of PTP1B was measured using 4-nitro-

phenylphosphate (pNPP) as a substrate. Progress of the enzymatic reaction was monitored at 405 nm by recording the absorption of the 4-nitrophenolate, the product of pNPP cleavage. The sodium salts of **4**–**6** showed no time-dependent inhibition at concentrations up to 20 mM, suggesting that the mono-*P*-fluorophosphonates did not act as irreversible inhibitors. Time-dependent inhibition of PTP1B, however, was observed when the acid forms of **1**–**6** were investigated in the same assay. This inhibitory effect disappeared at doubled buffer concentration (50 mM) and could be traced back to the deactivation of PTP1B at reduced pH values (see Figures S4–S6 in the Supporting Information). All measured fragments showed inhibitory constants in mM-range (Table 1).

Table 1. Inhibition of PTP1B with the phosphonates **1**, **2**, **3**, **7**, **9**, **11**, and the corresponding mono-*P*-fluorophosphonates **4**, **5**, **6**, **8**, **10**, and **12**. All compounds measured as mono sodium salts.

Cmp.	K_i [mM][a]	Ratio K_i(P–F)/K_i(P–O$^-$)
1	n.i.[b]	–
2	≈5	–
3	1.910 ± 0.228[c]	–
4	n.i.[b]	–
5	≈10	≈2
6	3.855 ± 0.349	2.02
7	0.101 ± 0.011	-
8	0.593 ± 0.047	5.87
9	0.164 ± 0.032	–
10	0.321 ± 0.063	1.96
11	0.060 ± 0.007[d]	–
12	0.081 ± 0.011	1.36

[a] Calculated with Cheng–Prusoff equation; error in standard deviation. [b] No inhibition. [c] Lit.: K_i = 2.5 mM ± 0.120.[40] [d] Reproducible value; reported in literature with an IC_{50} = 2.0 μM.[38]

To exclude the irreversible covalent reaction, we synthesized the mono-*P*-fluoro derivative of the fluorescein labeled phosphonate **7**. Considering that the direct fluorination of **7** would have affected the fluorophore as well, we synthesized the mono-*P*-fluorophosphonate **8** by prefluorination of the alkyne followed by Cu^I-catalyzed cycloaddition with a biotin azide and subsequent ion exchange. Potential covalent modifications of the phosphatase PTP1B after incubation with mono-*P*-fluoro phosphonates **8** were examined by gel electrophoresis looking for fluorescent protein bands (Figure 3).

The affinity of **7** and **8** was determined with K_i values of 101 μM for **7** and 593 μM for compound **8** respectively. The fluorescently labeled mono-*P*-fluorophosphonate **8** was then incubated at a concentration close to its binding constant with the protein for 1.5 h. No signs of covalent attachment of the probe **8** were detected in SDS-PAGE analysis. As a positive control STAT5B was photo-crosslinked with the fluorescein labelled benzoyl phosphonate peptide CF-K(Biotin)GpcFLSLPPW-NH_2 containing 4-phosphono-carbonyl phenylalanine (pcF) as the photoactive component.[18] A subsequently synthesized biotin-labeled mono-*P*-fluorophosphonate showed no response in anti-biotin Western blots. Thus, an irreversible covalent reaction was excluded.

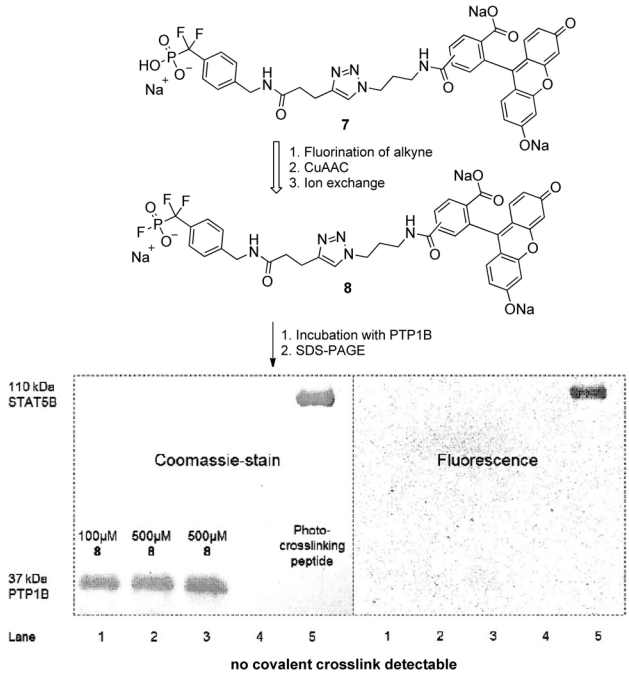

Figure 3. Synthesized mono-*P*-fluoro probe **8** incubated with PTP1B to evaluate a covalent modification of PTP1B; Lane 1: PTP1B incubated with **8** (c = 100 μM), Lane 2 and 3: PTP1B incubated with **8** (c = 500 μM), Lane 4: blank, Lane 5: STAT5B-MBP photo-crosslinked with peptide CF-K(Biotin)GpcFLSLPPW-NH_2 as a positive control.[18]

As a second potential mode of action, we assumed a covalent reaction with the active cysteine residue followed by the hydrolysis of the putative instable thioester intermediate. This should result in the formation of the starting material, the phosphonic acid, which could be monitored via ^{19}F NMR spectroscopy. For testing the substrate character we selected a 1:1 mixture of compound **6** and the corresponding phosphonic acid **3** to identify a hydrolysis reaction via the change in its ratio. The mixture was incubated with and without the active protein tyrosine phosphatase PTP1B in the very same assay buffer that is conventionally used for enzyme assays. NMR spectra were recorded after 14 h to detect enzyme-induced hydrolysis (Figure 4). No enzymatic cleavage of various tested compounds could be observed, not even with changing the buffer to HEPES and the protein tyrosine phosphatase to SHP2.

Thus, the experiments revealed that mono-*P*-fluorophosphonate **6** acted as reversible and (bio)-chemically stable inhibitor of PTP1B. Considering that the model compounds displayed only weak binding interactions to the protein, we decided to synthesize more potent inhibitors to evaluate the effect of the substitution of a negatively charged oxygen atom by fluorine over a broader range of binding affinities. To gain a representative view, two structures that differ by two magnitudes of affinity were selected (Scheme 2).[37,38] First, the naphthyl-substituted phosphonic acid **9** was synthesized, starting from 2-(bromomethyl)-naphthalene, which was reacted with triethyl phosphite, followed by electrophilic fluorination and hydrolysis after treatment with bromotrimethylsilane (TMSBr) (see the Supporting Information).

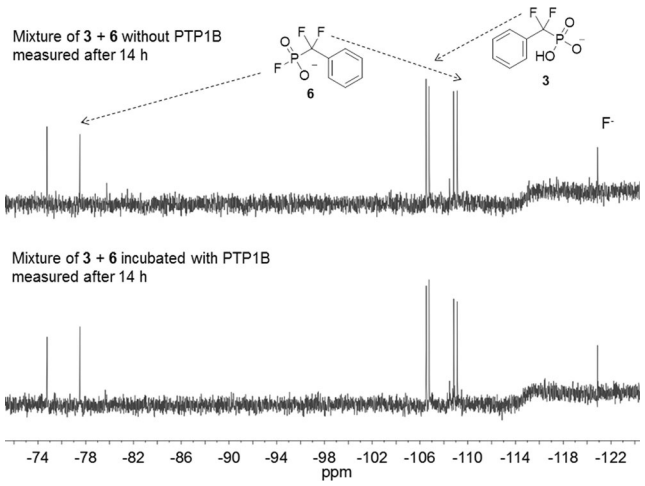

Figure 4. Evaluation of the enzymatic turn-over of mono-*P*-fluorophosphonate **6** as a substrate of PTP; ^{19}F NMR spectra of the mixture ($c = 4$ mM each) of **3** and **6** without (top) and with (bottom) incubation with PTP1B.

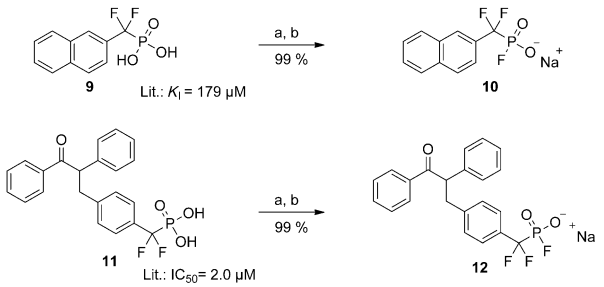

Scheme 2. Synthesis of the mono-*P*-fluorophosphonates **9** and **11** as stable phosphotyrosine mimetics.[37–38] Reaction conditions: a) $(COF)_2$, acetonitrile; b) 1. H_2O, 2. Na-Amberlite.

The mono-*P*-fluorinated phosphonate **10** was obtained after difluorination with oxalyl fluoride followed by hydrolysis and treatment with sodium-loaded Amberlite resin. Secondly, the phosphonic acid **11** based on a phenylacetophenone scaffold was synthesized (see the Supporting Information). Fluorination and ion exchange furnished the mono-*P*-fluorophosphonate **12**.

The synthesized phosphonates **1**, **2**, **3**, **7**, **9**, and **11** and their corresponding mono-P-fluorophosphonates **4**, **5**, **6**, **8**, **10**, and **12** were investigated as inhibitors of PTP1B using the pNPP assay. All compounds were reversible inhibitors. IC_{50} values were recorded and converted to the inhibitory constants K_I using the Cheng–Prusoff equation (Table 1).[39]

A measurable inhibitory effect of the benzyl-substituted compounds **1** and **4** was observed only at concentrations >30 mM. However, the data did not allow the determination of an inhibition constant for these compounds. The α-*C*-monofluorinated bioisosteres **2** and **5** inhibited PTP1B with K_I values around 5 and 10 mM, respectively, although the determination of K_I values at such high concentrations lacks precision. K_I values of the compound **3** and **6**–**12** were measured with high reproducibility and acceptable statistical deviation. When the affinities of the five mono-*P*-fluorophosphonates **5**, **6**, **8**, **10**, and **12** were compared with those of the respective phosphonic acids **2**, **3**, **7**, **9**, and **11,** affinity ratios of 2, 2.02, 5.87, 1.96, and 1.36 were determined (Table 1). Most pairs displayed an affinity ratio close to 2, both for the simple fragments **5** and **6** and for the stronger binding compounds **10** and **12**, suggesting that in these cases, the affinity constant of the fluoride is twice as high as those of the phosphonate. Only the fluorescently labeled probes **7** and **8** deviated from this regularity displaying an affinity ratio of 5.87. This observation could correspond to an increased binding of phosphonate **7**, possibly due to aggregation of this of this fluorescein-labeled, amphiphilic compound.

Considering the relation between the binding affinities and the free binding energies in a pair of compounds ($-RT\ \ln(K_{I1}/K_{I2}) = \Delta G_1 - \Delta G_2$), the observed affinity ratio of 2 corresponds at 20 °C to the difference in free binding energy $\Delta\Delta G$ of 1.7 kJ mol^{-1} between a bound phosphonate and its respective mono-*P*-fluoro-derivative. This difference in binding energy reflects the change in Coulomb interactions between a P–O^- residue and a P–F substituent and the cost in binding energy for the substitution of a dianionic species by that of a monoanion in this individual case. Although hydrogen bond pairing in protein–ligand interactions and its influence on binding affinities is a widely discussed and not well-understood topic,[41–45] a loss of free binding of only 1.7 kJ mol^{-1} for replacing a P–O^- residue by a P–F functionality appeared to be a moderate price and suggested the possibility of favorable interactions for the P–F residue with the phosphotyrosine binding pocket.

Synthesis and evaluation of α,α-difluorobenzyl-penta-*P*-fluorophosphate 13

Considering that the substitution of an O^- functionality with a fluorine atom resulted in stable and reversible inhibitors of the protein tyrosine phosphatase PTP1B with only a 2-fold decrease in affinity, we wondered whether the incorporation of additional fluorine substituents at the phosphorus might yield another phosphotyrosine mimetic. During attempts of synthesizing the mono-*P*-fluorinated phosphonate **6** via the treatment of the activated di-*P*-chloro phosphonate of **3** with alkaline fluorides, we observed the formation of a compound that showed a more complex ^{31}P–^{19}F-coupling. These signals corresponded to the heptafluorinated derivative **13**, α,α-difluorobenzyl-penta-*P*-fluorophosphate, which initially could not be isolated in a pure form and was obtained in a mixture with other organophosphorus species. NMR spectra indicated the coupling pattern of an octahedral coordination at the phosphorus atom with one axial and four equatorial fluorine atoms. HRMS measurements confirmed the pentafluorination at the phosphorus center. Placement of compound **13** in the active site of a published structure of the protein PTP1B with reference inhibitor **3**[35] led after energy minimization to a binding mode of the ligand **13** with numerous interactions exceeding those of the phosphonate **3** and of the mono-P-fluorophosphonate **6** (Figure 5). According to the molecular model, binding of **13** was accomplished by H-bonds from Cys215, Ser216,

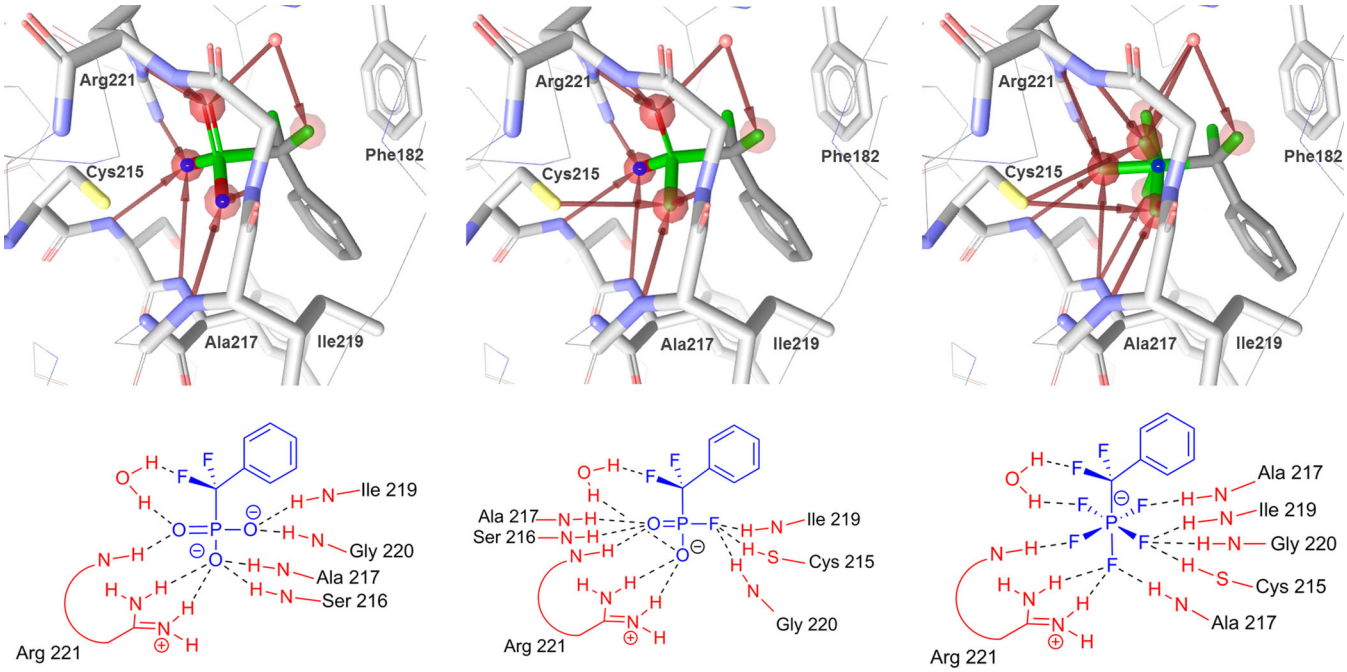

Figure 5. Calculated interactions of phosphonate **3**, the mono-*P*-fluorophosphonate **6** and Ph–CF_2–PF_5^- **13** (from left to right) PTP1B.[46] Based on the crystal structure from reference, PDB code: 4Y14 (Dimer B).[35]

Ile219, Gly220, and Arg221. Moreover, the protonated side chain of Arg221 was involved in charge interactions, while Tyr46, Val49, and Phe182 contributed to hydrophobic interactions.

On the basis of these favorable binding predictions, further effort was invested into developing a protocol for the synthesis and isolation of compound **13**.

As mentioned above, treatment of phosphonate **3** with oxalyl chloride followed by metal fluorides yielded mixtures of difluorobenzyl penta-*P*-fluorophosphate **13** with other compounds such as difluorobenzyl mono-*P*-fluorophosphonate **6**. This synthetic route, however, showed unsatisfying reproducibility in product formation and the isolation of compound **13** could not be accomplished. A much more reliable preparation of the $PhCF_2PF_5$-anion **13** was realized when tetramethylammonium fluoride (NMe_4F) was used as the source of fluoride (Scheme 3).[47]

Formation of α,α-difluorobenzyl-penta-*P*-fluorophosphate **13** was confirmed by HPLC-MS analysis displaying very uncommon elution properties both on C8 and C18 reverse-phase silica. Although the phosphonic acids **3** and **6** eluted at 3.4 and 5.2 min, respectively on RP-18 material, displaying symmetric peaks and characteristic UV spectra, compound **13** interacted strongly with the column material, resulting in elution after 9 min at the very end of the default gradient (5 to 95% CH_3CN in H_2O, see Figure S2 in the Supporting Information). Additionally, no absorbance of **13** at the wavelength 210 nm, 254 nm and 290 nm was observed. These properties hampered chromatographic purifications like reversed-phase MPLC and HPLC. Crystallization of **13** from the product fractions resulted in an overall yield of 21%. Subsequent NMR analysis clearly showed the octahedral coordination around the phosphorus nucleus (Figure 6).

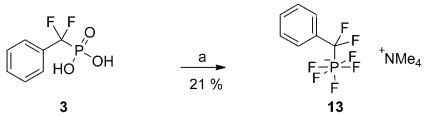

Scheme 3. Synthesis of the NMe_4-α,α-difluorobenzyl-penta-*P*-fluorophosphate **13**. Reaction conditions: a) 1. $(COCl)_2$, [DMF], DCM; 2. NMe_4F, acetonitrile.

In accordance with the elution properties on RP-HPLC, the tetramethylammonium α,α-difluorobenzyl pentafluoro phosphate **13** is significantly more lipophilic compared to phosphonate **3**, thus being more soluble in acetonitrile than in water.

The stability of pentafluorophosphate **13** was investigated over the pH range from 2 to 12 in aqueous solution using ^{19}F NMR spectroscopy in D_2O and no degradation or hydrolysis could be observed, also confirming the stability of **13** under physiological buffer conditions. Initial investigations of the inhibitory potential towards the protein tyrosine phosphatase PTP1B showed a significant affinity but insufficient reproducibility. In order to enhance the solubility in aqueous systems and to exclude any interfering effects of the counter ion NMe_4^+, we transferred compound **13** into its sodium salt **13-Na**. While showing the same characteristics during HPLC measurements, ion exchange resulted in an increased solubility of **13-Na** in water up to 200 mM without any loss in stability. Using the very same assay, the detection of the chromogenic *para*-nitrophenolate at 405 nM, we determined the inhibition constant K_i of product fractions from several synthetic batches in a final set of 187 data points as a value of 1.81 mM (Figure 7 A).

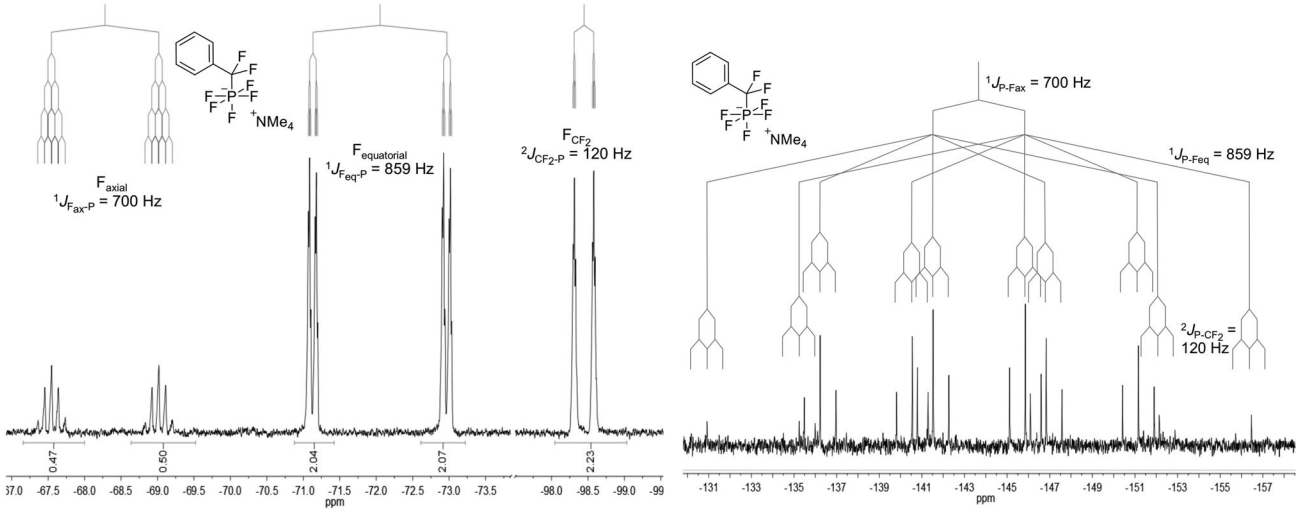

Figure 6. ^{19}F NMR (D_2O) (left) and ^{31}P NMR ([D6]DMSO) (right) spectra of the penta-*P*-fluorophosphate **13**.

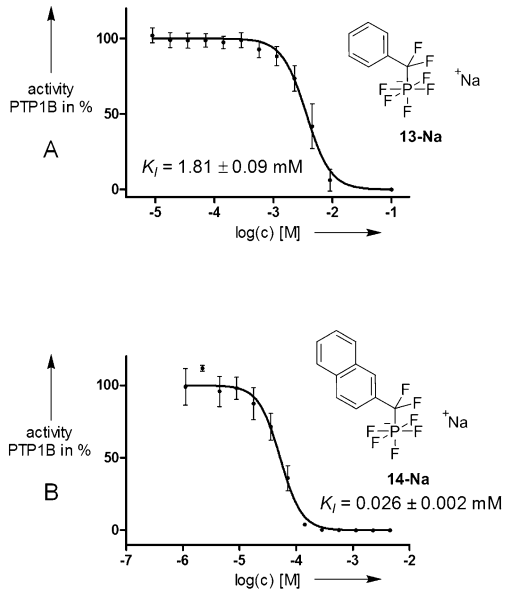

Figure 7. Inhibition of PTP1B at various concentrations of **13-Na** (A) and **14-Na** (B). In case of **13-Na** a data point with 100% inhibition was added at 100 mM concentration without altering the calculated K_I values.

During the measurements of the inhibitory effect of **13-Na**, inhibitors with known inhibition constants were used in parallel as positive controls to verify the reliability of the assay. The inhibition constant of 1.81 mM suggests equal or even more favorable protein-inhibitor interactions of the R–PF_5^- moiety than the phosphonate R–$P(O)O_2^{2-}$, which is present in compound **3** (K_I = 1.910 mM).

Next, we wanted to extend these findings to other penta-*P*-fluorophosphates. Pentafluorination of benzyl phosphonate **1** using a modified reaction protocol furnished a pentafluorinated product that decomposed at room temperature and thus was not suitable for biochemical studies.[48] Pentafluorination of the difluoro-naphth-2-yl-methylphosphonate **9**, however, afforded a heptafluorinated product **14-Na** which was stable and soluble in the biochemical buffer. The K_I of **14-Na** was determined as 0.026 mM, more than 6 times lower than the respective phosphonate **9** (0.164 mM).

These results corroborate that difluoro-methyl-pentafluorophosphate fragments are indeed bioisosteres and biomimetics of phosphate residues.

Conclusion

In this work, novel ligands of protein tyrosine phosphates were derived from known phosphonate-based PTP inhibitors through substitution of a negatively charged O-functionality bound to the phosphorus center by a fluorine atom. Benzyl-mono-*P*-fluorophosphonates were subsequently examined for their mode of action toward the protein tyrosine phosphatase PTP1B. Three different scenarios were hypothesized and tested: first, benzyl-mono-*P*-fluorophosphonates might undergo a covalent reaction with the enzyme acting A) as irreversible inhibitors of PTP1B or B) as substrates resulting in the hydrolysis of the covalent intermediate. Alternatively, they might interact with the enzyme non-covalently as chemically stable and reversible inhibitors (C).

Elucidation of the mode of action revealed that the benzyl-mono-*P*-fluorophosphonates **5**, **6**, **8**, **10**, and **12** acted as reversible, chemically stable inhibitors of PTP1B. No covalent modification of the protein was observed and no hydrolysis took place in the presence of active PTP1B. Pairwise comparison of the binding constants of mono-*P*-fluorophosphonates with the respective phosphonates revealed a reduction of the free binding energy $\Delta\Delta G$ of 1.7 kJ mol^{-1} by replacing a P-O^- with a P-F substituent. Considering that the P-O^- contributes to the binding of phosphonates through charge interactions and H-bonds, this moderate reduction of the free binding energy suggests that the P-F residue contributes to the binding of the mono-P-fluorophosphonates, presumably by establishing F–H-bonds with the protein's active site.

This observation prompted us to synthesize and test further fluorine-substituted phosphorus compounds as potential new phosphotyrosine mimetics. Difluoro-benzyl-penta-*P*-fluorophosphate **13** was prepared and found to be a stable compound in aqueous solutions over a broad pH range. As hypothesized the penta-*P*-fluorophosphate **13** was established as a novel phosphotyrosine mimetic and identified as a reversible inhibitor of the protein tyrosine phosphatase PTP1B with an affinity similar to the reference compound, α,α-difluoro-benzyl phosphonate **3**. In the case of the difluoro-naphth-2-yl-methyl phosphonate **9** this effect was even more pronounced. The pentafluorophosphate derivative **14-Na** was found to be an inhibitor of PTP1B that was more than six times more active than the respective phosphonate **9** (0.026 mM vs. 0.164 mM).

Further research will show whether PTP inhibitors derived from the novel phosphotyrosine mimetic **13** with their reduced negative charge density and increased hydrophobicity will be able to penetrate cells and are metabolically stable, possibly leading to potent protein tyrosine phosphatase inhibitors with activity in vivo.

Experimental Section

Materials and methods: All reactions were performed in typical glassware and if appropriate, under dry conditions using Schlenk technology. All chemicals were purchased from common suppliers and were used without any further purification, if not mentioned otherwise. NMR spectra were measured on the following spectrometers (Bruker, AV 300; Varian, Mercury 300 MHz; Varian, Mercury 400 MHz, JEOL, ECX 400; JEOL, ECP 500). Chemical shifts are given in ppm relative to the signal of the used deuterated solvent as internal and TFA as well as 85% H_3PO_4 as external standards. ESI-HRMS were recorded with an ESI-Q-TOF spectrometer (Agilent Technologies, 6550) coupled with a HPLC (Agilent Technologies, Infinity II 1290).

Oxalyl fluoride: Oxalyl fluoride was prepared according to literature.[36] Deviant from the existing preparation instructions, multiple distillation of oxalyl fluoride could not be accomplished without significant loss of the product. Considering that the published boiling points were given as ambiguous values and taken into account the hazardous potential of this compound, we dissolved the condensate of the first distillation in deuterated acetonitrile (1:3). Acetonitrile, besides toluene, was the only suitable solvent for a prolonged storage up to 2 weeks.

Sodium benzyl-mono-*P*-fluorophosphonate (4): Benzyl-di-*P*-fluoro phosphonate was prepared according to literature (see the Supporting Information).[49] The solidified difluoride was hydrolyzed in water followed by the addition of sodium-loaded Amberlite resin (weakly acidic, acetate-based). The mixture was stirred for 10 min, filtered and lyophilized to give **4** as a white solid in quantitative yield. ^{1}H NMR (300 MHz, D_2O): $\delta = 7.39$ (m, 5H, Ar), 3.21 ppm (dd, $J = 21.8$ Hz, $J = 3.9$ Hz, 2H, -CH_2-); ^{13}C NMR (75 MHz, D_2O): $\delta = 133.6$ (m), 129.7 (d, $J = 7.7$ Hz), 128.9 (d, $J = 3.2$ Hz), 126.7 (d, $J = 4.4$ Hz), 33.4 ppm (dd, $J = 136$ Hz, $J = 29.9$ Hz); ^{19}F NMR (282 MHz, D_2O): $\delta = -63.5$ ppm (dt, $J = 989$ Hz, $J = 3.9$ Hz); ^{31}P{^{1}H} NMR (162 MHz, D_2O): $\delta = 24.9$ ppm (d, $J = 990$ Hz); ESI-HRMS (*m/z*): $[M+H]^+$ calculated for $C_7H_9FO_2P^+$: 175.03187 Da; found: 175.03259.

General procedure for the fluorination with oxalyl fluoride: The corresponding phosphonic acid **2**, **3**, **9,** or **11** (10–20 mg) was dried under high vacuum, dissolved in a minimal amount of CD_3CN and cooled to −20 °C. Oxalyl fluoride dissolved in CD_3CN (1:3, 200 μL) was added through a syringe and the reaction mixture stirred for 2 h at −20 °C. The solvent and the excess of oxalyl fluoride were removed under a stream of nitrogen. Sodium loaded Amberlite® resin (Weakly Acidic Cation Exchanger, CG50) and water (1 mL) was added and the mixture warmed to room temperature. Filtration and lyophilization yielded the corresponding mono-*P*-fluorophosphonate as off-white powders.

Sodium mono-*P*-fluoro-(fluoro-(phenyl)-methyl)-phosphonate (5): m.p. >315 °C; Yield: 17 mg, 73%; ^{1}H NMR (400 MHz, D_2O): $\delta =$ 7.49 (m, 5H, Ar), 5.83 ppm (dd, $J = 44$ Hz, $J = 8$ Hz); ^{13}C NMR (126 MHz, D_2O): $\delta = 133.8$ (d, $J = 19$ Hz), 129.2 (br m), 128.7 (br m), 126.7 (br m), 89.1 ppm (br m); ^{19}F NMR (376 MHz, D_2O): $\delta =$ −70.4 ppm (dd, $J = 1019$ Hz, $J = 9$ Hz, P-*F*), −196.2 (ddd, $J = 85$ Hz, $J = 44$ Hz, $J = 9$ Hz, CH*F*); ^{31}P NMR (162 MHz, D_2O): $\delta = 12.9$ ppm (ddd, $J = 1019$ Hz, $J = 84$ Hz, $J = 8$ Hz); ESI-HRMS (*m/z*): $[M-H]^-$ calculated for $C_7H_6F_2O_2P^-$: 191.00790 Da; found: 191.00848.

Sodium mono-*P*-fluoro-(difluoro-(phenyl)-methyl)-phosphonate (6): m.p. >300 °C; Yield: 16 mg, 73%; ^{1}H NMR (400 MHz, D_2O): $\delta =$ 7.55 ppm (m, 5H); ^{13}C NMR (126 MHz, D_2O): $\delta = 130.9$ (br m), 130.3 (br m), 128.7 (br m), 128.4 (br m), 125.7 ppm (vbr m); ^{19}F NMR (376 MHz, D_2O): $\delta = -75.6$ (d, $J = 1036$ Hz, P-*F*), −108.4 ppm (d, $J =$ 115 Hz, CF_2); ^{31}P{^{1}H} NMR (162 MHz, D_2O): $\delta = 2.7$ ppm (dt, $J =$ 1036 Hz, $J = 114$ Hz); ESI-HRMS (*m/z*): $[M-H]^-$ calculated for $C_7H_5F_3O_2P^-$: 208.99847 Da; found: 208.99873.

Sodium mono-*P*-fluoro-(fluoresceinyl)-phosphonate (8): For synthesis see the Supporting Information. ESI-HRMS (*m/z*): $[M+H]^+$ calculated for $C_{37}H_{32}F_3N_5O_9P^+$: 778.18843 Da; found: 778.19087.

Sodium mono-*P*-fluoro-(difluoro-(naphth-2-yl)-methyl)-phosphonate (10): m.p. >315 °C; Yield: 9 mg, 99%; ^{1}H NMR (500 MHz, D_2O): $\delta =$ 8.21 (br s, 1H, H-1), 8.03 (m, 3H, H-4, H-5, H-8), 7.70 ppm (m, 3H, H-3, H-6, H-7); ^{13}C NMR (126 MHz, D_2O): $\delta = 133.6$, 132.2, 131.4 (td, $J = 22.1$ Hz, $J = 12.6$ Hz), 128.5, 128.3, 127.7, 127.5 (d, $J = 7.4$ Hz), 126.8 (d, $J = 7.4$ Hz), 126.0 (v br), 122.8 ppm (v br), the ^{19}F and ^{31}P coupled ^{13}C signal of -CF_2- was not resolved; ^{19}F NMR (376 MHz, D_2O): $\delta = -75.2$ (d, $J = 1037$ Hz), −107.9 ppm (d, $J = 115$ Hz); ^{31}P{^{1}H} NMR (162 MHz, D_2O): $\delta = 3.5$ ppm (dt, $J = 1037$ Hz, $J =$ 114 Hz); ESI-HRMS (*m/z*): $[M-H]^-$ calculated for $C_{11}H_7F_3O_2P^-$: 259.01412 Da; found: 259.01531.

Sodium mono-*P*-fluoro-4-((3-oxo-2,3-diphenylpropyl)-difluormethyl)-phosphonate (12): m.p. >315 °C; Yield: 12 mg, 99%; ^{1}H NMR (400 MHz, CD_3CN/ D_2O): $\delta = 7.64$ (d, $J = 7.7$ Hz, 2H, $H_{ortho,Ph\text{-}CO}$), 7.29 (d, $J = 8.0$ Hz, 2H, $H_{ortho,Ph\text{-}CF2}$), 6.99 (m, 8H), 6.85 (m, 2H), 4.79 (t, $J = 7.4$ Hz, 1H, -*CH*-), 3.27 (dd, $J = 13.7$ Hz, $J = 7.7$ Hz, 1H, $-CH_2-$), 2.86 ppm (dd, $J = 13.6$ Hz, $J = 7.8$ Hz, 1H, $-CH_2-$); ^{13}C NMR (176 MHz, D_2O): $\delta = 203.3$, 141.5, 138.4, 135.9, 133.8, 129.2, 129.0, 128.9, 128.7, 128.4, 127.4, 125.8, 120.0 (m), 54.7, 38.4 ppm; ^{19}F NMR (376 MHz, CD_3CN/D_2O, 1:1): $\delta = -74.1$ (d, $J = 1029$ Hz), −107.01 ppm (d, $J = 114$ Hz); ^{31}P{^{1}H} NMR (162 MHz, CD_3CN/D_2O): $\delta = 2.7$ ppm (dt, $J = 1028$ Hz, $J = 115$ Hz); ESI-MS (*m/z*): $[M+H]^+$ calculated for $C_{22}H_{19}F_3O_3P^+$: 419.10184 Da; found: 419.10190.

Tetramethylammonium (difluoro-(phenyl)-methyl)-penta-*P*-fluorophosphate (13): Compound **3** (460 mg, 2 mmol) and a catalytic amount of dry DMF were dissolved in dry DCM (4 mL). Oxalyl chloride (428.8 μL, 5 mmol, 2.5 equiv.) was added dropwise and the mixture heated to 40 °C and stirred for 2 hours at room temperature. The solvent and excess of $(COCl)_2$ were removed under reduced pressure and the residue dissolved in dry acetonitrile. NMe_4F (763 mg, 8.2 mmol, 4.1 equiv.) was added and the reaction was stirred 16 h at room temperature. The white precipitate was filtrated off, the filtrate was evaporated and purified by RP-MPLC (H_2O/ ACN, 5–99% acetonitrile). Lyophilization of the product frac-

tions afforded tetramethylammonium (difluoro-(phenyl)-methyl)-penta-*P*-fluorophosphate **13** as colorless crystals with light brown reflexes. Yield: 140 mg, 21%; m.p. 107 °C; ^{1}H NMR (400 MHz, [D6]DMSO): δ = 7.55 (d, J = 6.3 Hz, 1H), 7.44 (d, J = 6.8 Hz, 1H), 7.32 (ddd, J = 19.0 Hz, J = 10.9 Hz, J = 7.3 Hz, 3H), 3.09 ppm (s, 12H, N(CH_3)$_4$); ^{13}C NMR (101 MHz, [D6]DMSO): δ = 129.9, 128.3, 128.2, 127.6, 126.4, 125.7, 54.9 ppm; ^{19}F NMR (470 MHz, CD_3OD): δ = −67.7 (dp, J = 700 Hz, J = 46 Hz, 1F, F_{ax}), −69.9 (ddt, J = 858 Hz, J = 45 Hz, J = 8.6 Hz, 4F, F_{eq}), −97.3 ppm (ddt, J = 121 Hz, J = 17 Hz, J = 7.3 Hz, 2F, CF_2); ^{31}P NMR (162 MHz, [D6]DMSO): δ = −144 ppm (dtquin, J = 858 Hz, J = 700 Hz, J = 120 Hz); ESI-HRMS (m/z): [M]$^-$ calculated for $C_7H_5F_7P^-$: 253.0023; found: 253.0033.

Sodium (difluoro(phenyl)methyl)-penta-*P*-fluorophosphate (13-Na): Compound **13** was dissolved in water and treated with previously washed sodium-loaded Amberlite® resin. The obtained solution was subsequently eluted several times through syringes filled with the ion exchange resin. Completion of the ion exchange reaction was monitored by ^{1}H NMR through the loss of the NMe_4^+ signal.

Tetramethylammonium (difluoro-(naphth-2-yl)-methyl)-penta-P-fluorophosphate (14): Compound **9** (140 mg, 0.500 mmol) and a catalytic amount of dry DMF were dissolved in dry dichloromethane (1 mL). Oxalyl chloride (165.7 μL, 1.25 mmol, 2.5 equiv) was added dropwise, the mixture heated to 40 °C and stirred for 2 hours at room temperature. The solvent and excess of $(COCl)_2$ were removed under reduced pressure and the residue redissolved in dry acetonitrile (0.5 mL). NMe_4F (190.9 mg, 2.05 mmol, 4.1 equiv) was added and the reaction was stirred 16 h at room temperature. After filtration the solvent was removed under reduced pressure and the residue was washed twice with deionized H_2O. After drying under reduced pressure, tetramethylammonium (difluoro-(naphtha-2-yl)-methyl)-penta-*P*-fluorophosphate **14** was obtained as colorless crystals with light brown reflexes. Yield: 11 mg, 6%; m.p. 142 °C; ^{1}H NMR (700 MHz, CD_3OD/CD_3CN (7:1 (v/v))): δ = 7.95 (s, 1H, Ar), 7.90 (dd, J = 6.0, J = 3.4 Hz, 1H, Ar), 7.87 (dd, J = 6.1, J = 3.4 Hz, 1H, Ar), 7.83 (d, J = 8.7 Hz, 1H, Ar), 7.62 (d, J = 8.5 Hz, 1H, Ar), 7.50 (dq, J = 6.6, J = 3.5 Hz, 2H, Ar), 3.11 ppm (s, 12H, N(CH_3)$_4$); ^{13}C NMR (176 MHz, CD_3OD/CD_3CN): δ = 133.1, 132.5, 128.0, 127.2, 126.3, 125.8, 125.6, 124.0, 123.9, 116.9, 54.9 ppm; ^{19}F NMR (376 MHz, CD_3OD/CD_3CN): δ = −71.4 (dp, J = 696.5, J = 43.5 Hz, 1F, F_{ax}), −73.1 (ddt, J = 860.6, J = 44.3, J = 8.7 Hz, 4F, F_{eq}), −99.7 ppm (dt, J = 121.6, J = 16.7, J = 7.3 Hz, 2F, CF_2); ^{31}P NMR (162 MHz, CD_3OD/CD_3CN): δ = −143.2 ppm (dtquin, J = 860.5 Hz, J = 695.9 Hz, J = 121.7 Hz); ESI-HRMS (m/z): [M]$^-$ calculated for $C_{11}H_7F_7P^-$: 303.0179; found: 303.01772.

Sodium (difluoro-(naphth-2-yl)-methyl)-penta-P-fluorophosphate (14-Na): Compound **14** was dissolved in methanol and treated with previously washed sodium-loaded Amberlite® resin. The obtained solution was subsequently eluted several times through syringes filled with the ion exchange resin. Completion of the ion exchange reaction was monitored by ^{1}H NMR through the loss of the NMe_4^+ signal.

Acknowledgements

The authors acknowledge funding of the project by the SFB 765 (project B9) by granting a fellowship to M.A. We are grateful to Dr. Anja Schütz for providing the PTP1B.

Conflict of interest

The authors declare no conflict of interest.

Keywords: fluorine chemistry · fluorophosphates · fluorophosphonates · fragment-based drug discovery · phosphotyrosine mimetics · protein tyrosine phosphatases

[1] L. N. Johnson, *Biochem. Soc. Trans.* **2009**, *37*, 627–641.
[2] Á. González-Rodríguez, J. A. Mas Gutierrez, S. Sanz-González, M. Ros, D. J. Burks, Á. M. Valverde, *Diabetes* **2010**, *59*, 588–599.
[3] J. V. Olsen, B. Blagoev, F. Gnad, B. Macek, C. Kumar, P. Mortensen, M. Mann, *Cell* **2006**, *127*, 635–648.
[4] S. De Munter, M. Köhn, M. Bollen, *ACS Chem. Biol.* **2013**, *8*, 36–45.
[5] Y. A. Puius, Y. Zhao, M. Sullivan, D. S. Lawrence, S. C. Almo, Z.-Y. Zhang, *Proc. Natl. Acad. Sci. USA* **1997**, *94*, 13420–13425.
[6] A. Salmeen, J. N. Andersen, M. P. Myers, N. K. Tonks, D. Barford, *Mol. Cell* **2000**, *6*, 1401–1412.
[7] J. P. Sun, A. A. Fedorov, S. Y. Lee, X. L. Guo, K. Shen, D. S. Lawrence, S. C. Almo, Z. Y. Zhang, *J. Biol. Chem.* **2003**, *278*, 12406–12414.
[8] I. Marseigne, B. P. Roques, *J. Org. Chem.* **1988**, *53*, 3621–3624.
[9] M. S. Smyth, H. Ford Jr, T. R. Burke Jr, *Tetrahedron Lett.* **1992**, *33*, 4137–4140.
[10] T. R. Burke, M. S. Smyth, M. Nomizu, A. Otaka, P. R. Roller, *J. Org. Chem.* **1993**, *58*, 1336–1340.
[11] S. Grosskopf, C. Eckert, C. Arkona, S. Radetzki, K. Böhm, U. Heinemann, G. Wolber, J. P. von Kries, W. Birchmeier, J. Rademann, *ChemMedChem* **2015**, *10*, 815–826.
[12] K. Hellmuth, S. Grosskopf, C. T. Lum, M. Würtele, N. Röder, J. P. von Kries, M. Rosario, J. Rademann, W. Birchmeier, *Proc. Natl. Acad. Sci. USA* **2008**, *105*, 7275–7280.
[13] M. F. Schmidt, M. R. Groves, J. Rademann, *ChemBiochem* **2011**, *12*, 2640–2646.
[14] Y. Zhi, L. X. Gao, Y. Jin, C. L. Tang, J. Y. Li, J. Li, Y. Q. Long, *Bioorg. Med. Chem.* **2014**, *22*, 3670–3683.
[15] H. Zhao, G. Liu, Z. Xin, M. D. Serby, Z. Pei, B. G. Szczepankiewicz, P. J. Hajduk, C. Abad-Zapatero, C. W. Hutchins, T. H. Lubben, S. J. Ballaron, D. L. Haasch, W. Kaszubska, C. M. Rondinone, J. M. Trevillyan, M. R. Jirousek, *Bioorg. Med. Chem. Lett.* **2004**, *14*, 5543–5546.
[16] E. W. Yue, B. Wayland, B. Douty, M. L. Crawley, E. McLaughlin, A. Takvorian, Z. Wasserman, M. J. Bower, M. Wei, Y. Li, P. J. Ala, L. Gonneville, R. Wynn, T. C. Burn, P. C. C. Liu, A. P. Combs, *Bioorg. Med. Chem.* **2006**, *14*, 5833–5849.
[17] B. Douty, B. Wayland, P. J. Ala, M. J. Bower, J. Pruitt, L. Bostrom, M. Wei, R. Klabe, L. Gonneville, R. Wynn, T. C. Burn, P. C. C. Liu, A. P. Combs, E. W. Yue, *Bioorg. Med. Chem. Lett.* **2008**, *18*, 66–71.
[18] A. Horatscheck, S. Wagner, J. Ortwein, B. G. Kim, M. Lisurek, S. Beligny, A. Schütz, J. Rademann, *Angew. Chem. Int. Ed.* **2012**, *51*, 9441–9447; *Angew. Chem.* **2012**, *124*, 9577–9583.
[19] S. Wagner, A. Schütz, J. Rademann, *Bioorg. Med. Chem.* **2015**, *23*, 2839–2847.
[20] L.-C. Lo, Y.-L. Chiang, C.-H. Kuo, H.-K. Liao, Y.-J. Chen, J.-J. Lin, *Biochem. Biophys. Res. Commun.* **2004**, *326*, 30–35.
[21] Q. Zhu, X. Huang, G. Y. J. Chen, S. Q. Yao, *Tetrahedron Lett.* **2003**, *44*, 2669–2672.
[22] S. Kumar, B. Zhou, F. Liang, W. Q. Wang, Z. Huang, Z. Y. Zhang, *Proc. Natl. Acad. Sci. USA* **2004**, *101*, 7943–7948.
[23] S. Liu, B. Zhou, H. Yang, Y. He, Z. X. Jiang, S. Kumar, L. Wu, Z. Y. Zhang, *J. Am. Chem. Soc.* **2008**, *130*, 8251–8260.
[24] K. A. Kalesh, L. P. Tan, K. Lu, L. Gao, J. Wang, S. Q. Yao, *Chem. Commun.* **2010**, *46*, 589–591.
[25] K. Lee, H. Jin Kang, Y. Xia, S. J. Chung, *Anticancer Agents Med. Chem.* **2011**, *11*, 54–63.
[26] S. W. Wiener, R. S. Hoffman, *J. Intensive Care Med.* **2004**, *19*, 22–37.
[27] F. R. Sidell, J. Borak, *Ann. Emerg. Med.* **1992**, *21*, 865–871.
[28] S. Royo, R. Martínez-Mañez, F. Sancenón, A. M. Costero, M. Parra, S. Gil, *Chem. Commun.* **2007**, 4839–4847.

[29] Y. Liu, M. P. Patricelli, B. F. Cravatt, *Proc. Natl. Acad. Sci. USA* **1999**, *96*, 14694 – 14699.
[30] G. C. Adam, *Mol. Cell. Proteomics* **2002**, *1*, 781 – 790.
[31] B. Cravatt, *Curr. Opin. Chem. Biol.* **2000**, *4*, 663 – 668.
[32] S. A. Sieber, B. F. Cravatt, *Chem. Commun.* **2006**, 2311 – 2319.
[33] C. Meyer, B. Hoeger, K. Temmerman, M. Tatarek-Nossol, V. Pogenberg, J. Bernhagen, M. Wilmanns, A. Kapurniotu, M. Köhn, *ACS Chem. Biol.* **2014**, *9*, 769 – 776.
[34] Y. Han, M. Belley, C. I. Bayly, J. Colucci, C. Dufresne, A. Giroux, C. K. Lau, Y. Leblanc, D. McKay, M. Therien, M.-C. Wilson, K. Skorey, C.-C. Chan, G. Scapin, B. P. Kennedy, *Bioorg. Med. Chem. Lett.* **2008**, *18*, 3200 – 3205.
[35] N. Krishnan, K. Krishnan, C. R. Connors, M. S. Choy, R. Page, W. Peti, L. Van Aelst, S. D. Shea, N. K. Tonks, *J. Clin. Invest.* **2015**, *125*, 3163 – 3177.
[36] K. Takata, M. Takesue, Y. Iseki, T. Sata, *J. Fluorine Chem.* **1995**, *75*, 163 – 167.
[37] T. R. Burke, Jr., B. Ye, X. Yan, S. Wang, Z. Jia, L. Chen, Z. Y. Zhang, D. Barford, *Biochemistry* **1996**, *35*, 15989 – 15996.
[38] C. Dufresne, P. Roy, Z. Wang, E. Asante-Appiah, W. Cromlish, Y. Boie, F. Forghani, S. Desmarais, Q. Wang, K. Skorey, D. Waddleton, C. Ramachandran, B. P. Kennedy, L. Xu, R. Gordon, C. C. Chan, Y. Leblanc, *Bioorg. Med. Chem. Lett.* **2004**, *14*, 1039 – 1042.
[39] C. Yung-Chi, W. H. Prusoff, *Biochem. Pharmacol.* **1973**, *22*, 3099 – 3108.
[40] Z.-J. Yao, B. Ye, X.-W. Wu, S. Wang, L. Wu, Z.-Y. Zhang, T. R. Burke Jr, *Bioorg. Med. Chem.* **1998**, *6*, 1799 – 1810.
[41] D. Chen, N. Oezguen, P. Urvil, C. Ferguson, S. M. Dann, T. C. Savidge, *Sci. Adv.* **2016**, *2*, e1501240.
[42] H. Kubinyi, in *Pharmacokinetic Optimization in Drug Research*, Helvetica Chimica Acta, **2007**, pp. 513 – 524.
[43] V. Lafont, A. A. Armstrong, H. Ohtaka, Y. Kiso, L. Mario Amzel, E. Freire, *Chem. Biol. Drug Des.* **2007**, *69*, 413 – 422.
[44] A. M. Davis, S. J. Teague, *Angew. Chem. Int. Ed.* **1999**, *38*, 736 – 749; *Angew. Chem.* **1999**, *111*, 778 – 792.
[45] J. D. Chodera, D. L. Mobley, *Annu. Rev. Biophys.* **2013**, *42*, 121 – 142.
[46] G. Wolber, T. Langer, *J. Chem. Inf. Model.* **2005**, *45*, 160 – 169.
[47] N. V. Pavlenko, L. A. Babadzhanova, I. I. Gerus, Y. L. Yagupolskii, W. Tyrra, D. Naumann, *Eur. J. Inorg. Chem.* **2007**, 1501 – 1507.
[48] Conversion into the desired product was confirmed by ^{19}F NMR but could only be observed at reaction temperatures below $-10\,^{\circ}C$. Storage at room temperature and air led to a complete decomposition.
[49] R. Bender, C. Demay, J.-C. Elkaim, J. G. Riess, *Phosphorus Relat. Group V Elem.* **1974**, 183 – 186.

Manuscript received: March 17, 2017
Version of record online: ■■ ▮▮, 0000

FULL PAPER

Fluorophosphates

*S. Wagner, M. Accorsi, J. Rademann**

■■ – ■■

Benzyl Mono-*P*-Fluorophosphonate and Benzyl Penta-*P*-Fluorophosphate Anions Are Physiologically Stable Phosphotyrosine Mimetics and Inhibitors of Protein Tyrosine Phosphatases

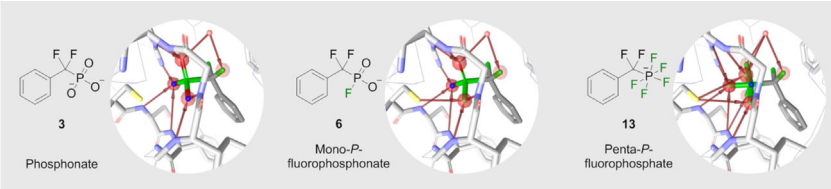

Through decades, phosphonates like **3** have constituted classical inhibitors of protein tyrosine phosphatases mimicking the favorable interactions of phenyl phosphate substrates while being non-hydrolyzable. Despite their popularity, phosphonates were not developed as drugs, yet, mainly due to severe issues in cell penetration. Here, modifications of this traditional class of inhibitors are presented by substituting P-bonded oxygen atoms with one (**6**) or five fluorine atoms (**13**).